Fate of rice shoot and root residues, rhizodeposits, and microbe-assimilated carbon in paddy soil: I. Decomposition and priming effect

Zhenke Zhu[1,2,#], Guanjun Zeng[2,#], Tida Ge[1,2], Yajun Hu[1], Chengli Tong[1], Olga Shibistova[3,4], Xinhua He[5], Juan Wang[1], Georg Guggenberger[1,3], and Jinshui Wu[1,2]

[1]Key Laboratory of Agro-ecological Processes in Subtropical Region, Institute of Subtropical Agriculture, Chinese Academy of Sciences, Hunan, 410125, China

[2]Changsha Research Station for Agricultural and Environmental Monitoring, Institute of Subtropical Agriculture, Chinese Academy of Sciences, Hunan, 410125, China

[3]Institute of Soil Science, Leibniz Universität Hannover, 30419 Hannover, Germany

[4]VN Sukachev Institute of Forest, Siberian Branch, Russian Academy of Science, 660036 Krasnoyarsk, Russian Federation

[5]College of Resources and Environment, Southwest University, Chongqing 400715, China.

# These authors contributed equally to this work.

Correspondence to: Tida Ge (gtd@isa.ac.cn) and Jinshui Wu (jswu@isa.ac.cn)

19   **Abstract.** The input of recently photosynthesized C has significant implications on soil organic C

20   sequestration, and in paddy soils, both plants and soil microbes contribute to the overall C input. In the

21   present study, we investigated the fate and priming effect of organic C from different sources by

22   conducting a 300-d incubation study with four different ^{13}C-labelled substrates: rice shoots (Shoot-C),

23   rice roots (Root-C), rice rhizodeposits (Rhizo-C), and microbe-assimilated C (Micro-C). The efflux of

24   both $^{13}CO_2$ and $^{13}CH_4$ indicated that the mineralization of C in Shoot-C-, Root-C-, Rhizo-C-, and

25   Micro-C-treated soils rapidly increased at the beginning of the incubation and then decreased gradually

26   afterwards. The highest cumulative C mineralization was observed in Root-C-treated soil (45.4%),

27   followed by Shoot-C- (31.9%), Rhizo-C- (7.9%), and Micro-C-treated (7.7%) soils, which

28   corresponded with mean residence times of 39.5, 50.3, 66.2, and 195 d, respectively. Shoot and root

29   addition increased C emission from native SOC, up to 11.4 and 2.3 times higher than that of the control

30   soil by day 20, and decreased thereafter. Throughout the incubation period, the priming effect of

31   Shoot-C on CO_2 and CH_4 emission was strongly positive; however, Root-C did not exhibit a significant

32   positive priming effect. Although the total C contents of Rhizo-C- (1.89%) and Micro-C-treated soils

33   (1.90%) were higher than those of untreated soil (1.81%), no significant differences in cumulative C

34   emissions were observed. Given that about 0.3% and 0.1% of the cumulative C emission were derived

35   from labelled Rhizo-C and Micro-C, we concluded that the soil organic C-derived emissions were

36   lower in Rhizo-C- and Micro-C-treated soils than in untreated soil. This indicates that rhizodeposits

37   and microbe-assimilated C could be used to reduce the mineralization of native soil organic C and to

38   effectively improve soil C sequestration. The contrasting behaviour of the different photosynthesized C

39   substrates suggests that recycling rice roots in paddies is more beneficial than recycling shoots and

40   demonstrates the importance of increasing rhizodeposits and microbe-assimilated C in paddy soils *via*

41   nutrient management.

42

43   **Keywords:** Paddy soil; Rice; Plant residues; Rhizodeposits; Microbe-assimilated carbon; CO_2 and

44   CH_4 emission; Priming effect

45

1 Introduction

The soils of rice paddies, which cover an area of ~165 million ha worldwide, hold great potential for expanded C sequestration (Conrad et al., 2012; Ge et al., 2012; Lal, 2004), and the soil organic carbon (SOC) pools in agricultural systems, of which plant C is the primary substrate, are significantly affected by the input of crop residues (Weintraub et al., 2007). For example, after crops are harvested or die, aboveground biomass, such as straw, stubble, and other surface debris, contribute to annual C inputs (Lu et al., 2003), and photosynthesized C substrates are continuously released by rice plants as rhizodeposits throughout the growing season (Lu et al., 2002, 2003). Furthermore, autotrophic soil microbes that assimilate CO_2 contribute to C sequestration in paddy soil as well (Ge et al., 2013; Yuan et al., 2012a), and since C inputs promote microbial activity and native SOC decomposition (Ye et al., 2015), their quantity and quality influence microbe-mediated decomposition processes (Brant et al., 2006; Creamer et al., 2015). Therefore, the quantification of different C substrates deposited in paddy soils and their respective effects on native SOC require further investigation.

The aboveground biomass and root systems of rice plants represent one of the most important inputs of available organic C to paddy SOC (Johnson et al., 2006), the quantity and quality of which has been reported previously (Chen et al., 2014; Kisselle et al., 2001; Zhang et al., 2015). However, although aboveground biomass contributes significantly to SOC sequestration (Lu et al., 2003), rice roots have been reported to contribute from 1.5- to 3-fold more C to SOC than shoots (Hooker et al., 2005). Similarly, Molina et al. (2001) emphasized that the stalks and leaves of corn contribute 50% less C to SOC than the roots and rhizodeposits. The predominant contribution of crop roots to SOC can partly be explained by the chemical composition of roots, which includes cellulose and lignin, as well as by residue-soil interactions, such as aggregate formation, which physically protect organic C from biodegradation (Baumann et al., 2009; Johnson et al., 2006; Lu et al., 2003).

Previous studies have also reported that the rhizodeposits of rice account for ~17% of the photo-assimilates (Nguyen, 2003) that enter paddy soil and that rice rhizodeposits include soluble exudates, root border cells, dead debris, and insoluble mucilage (Lu et al., 2003). In cereal crops, 10–25% of root exudates are incorporated into SOC, and rhizodeposits are thought to play a key role in C cycling and sequestration in plant-soil-microbe systems (Kuzyakov, 2002; Kuzyakov et al., 2003). In addition to the photosynthesized C substrates of plants, soil microbes are also able to assimilate CO_2

75   *via* the Calvin-Benson-Bassham cycle and, thus, can significantly contribute to the net uptake and

76   assimilation of atmospheric CO_2 as well (Ge et al., 2013; Yuan et al., 2012b). In fact, the CO_2 uptake

77   by phototrophic soil microbes has been reported to account for up to 0.36% of the total C fixed in rice

78   paddy soils and 0.19% of the total C fixed in upland soils (Ge et al., 2013; Yuan et al., 2012b).

79   So far, the effect of C input from different C sources on the balance and stability of SOC has

80   received limited attention. For example, the C in roots and shoots occur as particulate matter and must

81   be first depolymerized before being taken up by microorganisms, whereas rhizodeposits are

82   immediately available for uptake and assimilation by microorganisms, which is an important step in the

83   formation of stable organic matter (Kuzyakov, 2002; Kuzyakov et al., 2003). As low molecular weight

84   substances, rhizodeposits are also protected from mineralization *via* adsorption onto soil particles

85   (Jones and Edwards, 1998; Saidy et al. 2012; Sodano et al. 2016), which contributes to the stability

86   and sequestration of SOC (Ge et al., 2012). In addition, different C substrates can also have stimulating

87   or restraining effects on the mineralization of native SOC, which are known as positive or negative

88   priming effects (PEs), respectively (Kuzyakov, 2010). Priming is often caused by the addition of

89   substrates with relatively high C availability and nutrient contents, which results in increased microbial

90   activity (Blagodatsky et al., 2010; Huo et al., 2013). Hence, such easily degraded compounds greatly

91   enhance the decomposition of native SOC (Blagodatsky et al., 2007; Qiao, et al., 2014), compared with

92   the effects of ryegrass, cellulose, or wheat straw, which have more complex structures that are less

93   available to microbes (Kuzyakov and Bol, 2006; Kuzyakov et al., 2000). However, since easily

94   available low molecular weight substrates, such as rhizodeposits, can be easily immobilized by

95   microbial metabolism (Lu et al., 2002; Gunina et al., 2014) or adsorption (Jones and Edwards, 1998;

96   Saidy et al. 2012; Sodano et al. 2016), their PE can be small or even negative (Ge et al., 2012).

97   Accordingly, the quantity and quality of different C inputs, as well as their fate and PE in paddy

98   soils, are globally important (Bastida et al., 2013; Johnson et al., 2006; Wang et al., 2015). However,

99   few studies have investigated the fate of plant residues and rhizodeposits in paddy soils, and to the best

100   of our knowledge, there is no comparative information on the decomposition of different organic C

101   sources, such as rice shoots and roots, rhizodeposits, and microbe-assimilated C or on the effects of

102   different organic C sources on the mineralization of native SOC. Therefore, the aim of the present

103   study was to investigate the fate and priming effect of organic C from different sources. We

hypothesized that both the decomposition of organic C sources and their PE on the decomposition of native soil organic matter varies, depending on the type of organic C. We assumed that, since shoots and roots enter the soil as unprotected particulate organic residues, both substrates are readily available for microorganisms and that, as a result, such residues should also stimulate the decomposition of native organic matter; whereas rhizodeposits and microbial C represent C sources that can be better stabilized and thus contribute less to priming. We investigated these hypotheses by quantifying the contribution of different organic C sources to CO_2 and CH_4 emissions and by analysing their PEs during a 300-d incubation study, using ^{13}C-labelled rice plant residues, rhizodeposits, and microbe-assimilated C in paddy soils.

2   Materials and methods

2.1 Study site and soil sampling

The experimental rice field was located at the Changsha Research Station for Agricultural and Environmental Monitoring, Hunan, China (113°19′52″ E, 28°33′04″ N; 80 m above sea level), where the climate is subtropical, with a mean annual temperature and rainfall of 17.5 ℃ and 1300 mm, respectively. The soil developed from highly weathered granite and is classified as a typical Stagnic Anthrosol, Moist soil samples were collected from the plough layer (0–20 cm) and sieved (<4 mm) to remove visible plant residues. The soil contained 18.1 g kg^{-1} organic C with a δ^{13}C value of -26.7‰, 1.8 g kg^{-1} total N, and 0.4 g kg^{-1} total K and had a pH of 5.6 at a soil:water ratio (w/v) of 1:2.5.

2.2 Production of ^{13}C-labelled substrates

Rice cultivation and ^{13}CO$_2$ labelling were performed as described by Ge et al. (2012; 2013), with some modifications. Briefly, 60 pots were filled with 1 kg dry soil, and of these, 40 pots were planted with three 30 d old rice seedlings (*Oryza sativa* L. 'Zhongzao 39') each, whereas the remaining 20 pots were unplanted.

For ^{13}C labelling, 20 planted and 10 unplanted pots were transferred to an automatically controlled gas-tight growth chamber (110 cm length, 250 cm width, 180 cm height) and exposed to ^{13}CO$_2$-fumigation for 18 d (May 14–31, 2013), during the vegetative growth period (including the entire tillering stage). The growth chambers were placed in a rice field to ensure that the environmental

conditions of the labelled and control plants would be identical for labelled plants and unlabelled controls. The remaining 30 pots (20 planted, 10 unplanted), which served as controls for measuring natural ^{13}C abundance, were placed 10–15 m from the growth chambers. The water surface of each planted pot was covered with black plastic sheeting, to prevent algal photosynthesis in the floodwater and to ensure that only the rice shoots were exposed to $^{13}CO_2$, whereas the unplanted pots were left uncovered, so that the soils were directly exposed to $^{13}CO_2$ and so phototrophic soil microbes could assimilate atmospheric $^{13}CO_2$. All the pots were watered every few days, in order to maintain a water depth of 2–3 cm above the soil surface, until harvest. Weeds were removed manually.

The CO_2 concentrations of the growth chambers were measured using an infrared analyser (Shsen-QZD, Qingdao, China) and maintained at 360–380 μl L^{-1}. The $^{13}CO_2$ was generated by acidifying Na$_2$^{13}CO$_3$ (1.0 M, 99 atom % ^{13}C; Cambridge Isotope Laboratories, Tewksbury, MA, USA) with H$_2$SO$_4$ (0.5 M) in beakers that were placed inside the growth chambers. During the labelling period, $^{13}CO_2$ was only released when CO_2 concentrations fell below 360 μl L^{-1}, and at CO_2 concentrations >380 μl L^{-1}, the gas flow was diverted and passed through CO_2 traps (NaOH solution). An air-conditioning system was used to control the temperature inside the chamber within 1 ℃ of the ambient temperature in the rice field. Two fans continuously circulated the air in the growth chamber.

2.3 ^{13}C-labelled substrate collection

All the rice plants and soils were sampled destructively after 18 d of $^{13}CO_2$ labelling. Rice shoots were removed at their bases, whereas rice roots were separated from the soil by washing with deionized water, and both shoots and roots were dried at 60 ℃ for 48 h and then cut into <5 mm pieces. To collect ^{13}C-labelled rhizodeposits, moist soil was removed from the rice roots by gently shaking, and the soil adhering to the roots collected by washing the roots with distilled water. Subsequently, the resulting soil slurries were mixed and centrifuged at 13,000 × g for 15 min. The low-density fine roots were removed, along with the supernatants, whereas the rhizodeposits were collected with the soil. To obtain microbe-assimilated ^{13}C, we collected soil from ^{13}C-treated, unplanted pots and mixed it thoroughly.

2.4 Soil incubation

162   To determine the PEs of different C sources and the effect of different C substrates on CO_2 and CH_4

163   emission, we conducted a 300-d incubation study of paddy soils that had been supplemented with

164   ^{13}C-labelled shoots, roots, rhizodeposits, or microbe-assimilated C. Five treatments were used: (1)

165   unlabelled and unplanted paddy soil supplemented with ^{13}C-labelled shoot residue (Shoot-C), (2)

166   unlabelled and unplanted paddy soil supplemented with ^{13}C-labelled root residue (Root-C), (3) soil

167   containing ^{13}C-labelled rhizodeposits (Rhizo-C), (4) ^{13}C-labelled soil containing ^{13}C-labelled

168   microbe-assimilated C (Micro-C), and (5) unlabelled and unplanted soil without supplementation (CK).

169   Three additional treatments were used to determine the natural abundance of [13]C: (1) unlabelled and

170   unplanted paddy soil with unlabelled shoot residue, (2) unlabelled and unplanted paddy soil with

171   unlabelled root residue, and (3) unlabelled and unplanted paddy soil with unlabelled rhizodeposits.

172   For the Shoot-C and Root-C treatments, 150 g (100 g dry weight equivalent) unlabelled,

173   unplanted soil with a water content of 50% was homogenized with 0.6 g of labelled and dried shoot and

174   root residue, respectively, with a final residue content of 6 g kg^{-1}. Subsequently, the samples were

175   transferred to 500 ml serum bottles with 100 ml deionized water, to ensure a water layer of 2–3 cm, and

176   the bottles were sealed with butyl rubber stoppers. For the Rhizo-C and Micro-C treatments, 150 g

177   fresh soil containing either ^{13}C-labelled rhizodeposits (from rice roots) or ^{13}C-labelled

178   microbe-assimilated C (from labelled, unplanted pots) were directly weighed into 500 ml serum bottles,

179   respectively. Incubation was conducted at 25 ℃ in the dark for 300 d, with four replicates for each

180   treatment. CH_4 and CO_2 concentrations of the headspace samples were collected at 1, 3, 5, 10 d and

181   then every 10 d after sealing, the gas was collected using a gas-tight syringe and stored in

182   pre-evacuated Exetainer glass bottles (Labco, High Wycombe, UK). After each sampling point, the

183   serum bottle was ventilated for 10 min, and then sealed with butyl rubber stoppers.

184

185   **2.5 Analytical methods**

186   The C content of the soil and plant residues (shoots and roots) was determined using dry combustion

187   with an elemental analyser (vario MAX; Elementar Analysensysteme GmbH, Hanau, Germany),

188   whereas the CH_4 and CO_2 concentrations of the headspace samples were measured using a gas

189   chromatograph (Agilent 7890A, Agilent Technologies, Alto Palo, California, USA) equipped with a

190   thermal conductivity detector for measuring CO_2 and a flame ionization detector for measuring CH_4. In

191   addition, the stable C isotope composition of soils and plant residues were analysed using an isotope

192   ratio mass spectrometer coupled with an elemental analyser (FLASH 2000; Thermo Fisher Scientific,

193   Waltham, MA, USA), whereas the stable C isotope composition of CO_2 and CH_4 in the headspace

194   samples were analysed using the isotope ratio mass spectrometer coupled with a GasBench (Thermo

195   Fisher Scientific, Waltham, MA, USA).

196

197   **2.6 Calculations and statistical analysis**

198   The $\delta^{13}C$ values of plant residues, rhizodeposits, microbe-assimilated C, soils, CO_2, and CH_4 were

199   converted to δ (‰), relative to the Pee Dee Belemnite (PDB, 0.0111802) standard and were then

200   expressed in atom%, as follows:

201
$$\text{atom\%} = \frac{100 * 0.0111802 * (\frac{\delta}{1000} + 1)}{1 + 0.0111802 * (\frac{\delta}{1000} + 1)}. \tag{1}$$

202   Meanwhile, the incorporation of excess ^{13}C in plant residues, rhizodeposits, microbe-assimilated C,

203   bulk soils, CO_2, and CH_4 was calculated as follows:

204
$$\text{excess } ^{13}C_{sample} = [(\text{atom\%}^{13}C)_L - (\text{atom\%}^{13}C)_{UL}] \times C_{sample}/100, \tag{2}$$

205   where *(atom% ^{13}C)*$_L$ and *(atom% ^{13}C)*$_{UL}$ indicate the *atom% ^{13}C* in labelled and unlabelled samples,

206   respectively, and C_{sample} represents the C contents of each sample.

207   The $^{13}CO_2$ and $^{13}CH_4$ efflux (%) were calculated as the increases in excess ^{13}C-CO_2 and ^{13}C-CH_4

208   within each sampling interval, respectively, as percentages of the ^{13}C input. The mineralization

209   percentage of the input ^{13}C was calculated as the sum of total ^{13}C in CO_2 and CH_4, at each sampling

210   day, relative to the initially added total ^{13}C.

211   The kinetics of the mineralization were described by fitting a first order single exponential

212   function:

213
$$y = a\left(1 - e^{-bx}\right), \tag{3}$$

214   where *a* describes the amount of bioavailable labelled-substrate pool; *b* is the mineralization rate of the

215   substrate; and *x* is time (d). Obtained parameters were used to calculate the mean residence time as $1/b$

216   and half-life as $\ln(2)/b$.

217   The end-member mixing model was used to calculate the fractions of SOC- (C_{SOC}) and plant

218   residue-derived C (C_{shoot} and C_{root}), as described by Phillips et al. (2005) and Wild et al. (2014). This

219　model allows the combination of mass spectrometric and efflux measurements. The shoot-derived

220　$^{13}CO_2$ emission ($^{13}CO_{2shoot\text{-}derived}$) was calculated as follows:

221
$$^{13}CO_{2shoot\text{-}derived} = \frac{atom\%\ CO_{2shoot} - atom\%\ CO_{2CK}}{atom\%\ C_{shoot} - atom\%\ C_{soil}} \times CO_{2shoot\text{-}C}, \qquad (4)$$

222　where $atom\%\ CO_{2shoot}$ and $atom\%CO_{2CK}$ are the $atom\%\ ^{13}C$ values of CO_2 derived from

223　Shoot-C-treated soil and untreated soil (CK), respectively; $atom\%C_{shoot}$ and $atom\%C_{soil}$ are the $atom\%$

224　^{13}C values of Shoot-C-treated and bulk soil, respectively; and $CO_{2shoot\text{-}C}$ is the total CO_2 derived from

225　shoot treated soil. The shoot-derived $^{13}CH_4$ emission ($^{13}CH_{4shoot\text{-}derived}$) and the root-derived $^{13}CO_2$ and

226　$^{13}CH_4$ emission ($^{13}CO_{2root\text{-}derived}$ and $^{13}CH_{4root\text{-}derived}$, respectively) were calculated similarly (Phillips et

227　al., 2005; Ye et al., 2015).

228　　　The PE of SOM on CO_2 and CH_4 emission was calculated as follows:

229
$$PE_t(\%) = \frac{Gas - Gas_{CK}}{Gas_{CK}} \times 100, \qquad (5)$$

230　where PE_t is the PE at time t (d); Gas the total amount of CO_2 and CH_4 derived from native SOC

231　mineralization in the treatment of Shoot-C and Root-C, and Gas_{CK} is the SOC mineralization in the CK

232　treatment (Hu et al., 2012).

233　　　Analysis of variance in conjunction with Duncan's multiple range test ($p < 0.05$) and correlation

234　analysis were conducted using SPSS 17 (SPSS Inc., Chicago, IL, USA), and figures were created using

235　Origin 8.5 (OriginLab, Northampton, MA, USA).

236

237　3　Results

238　3.1 CO_2 and CH_4 emission of carbon substrate-treated soils

239　　　The excess ^{13}C per 100 g soil was 11.4, 5.75, 1.61, and 0.49 mg in the Shoot-C, Root-C, Rhizo-C,

240　and Micro-C treatments, respectively (Table 1). The $^{13}CO_2$ efflux from the each treatment increased

241　rapidly at the beginning of the incubation, peaked after 20 d, and then decreased gradually (Fig. 1a).

242　The CO_2 efflux rates from the Shoot-C- and Root-C-treated soils were 0.71 and 0.66% of the initial ^{13}C

243　per day, respectively, which was higher than those of Rhizo-C- (0.11% of initial ^{13}C per day) and

244　Micro-C-treated (0.06% of initial ^{13}C per day) soils. The $^{13}CH_4$ efflux rates exhibited similar patterns

245　(Fig. 1b). The cumulative $^{13}CO_2$ and $^{13}CH_4$ emissions increased strongly during the first 60 d of

246　incubation, after which they increased more slowly (Fig. 2). The total $^{13}CO_2$ emissions accounted for

247   28.6 and 43.8% of the initial ^{13}C from Shoot-C and Root-C, respectively, and 7.9 and 7.7% of the

248   initial ^{13}C from Rhizo-C and Micro-C (Fig. 2a). The cumulative $^{13}CH_4$ emissions only accounted for

249   3.3 and 1.6% of the initial ^{13}C from Shoot-C and Root-C, respectively, whereas no $^{13}CH_4$ was detected

250   in the emission of the Rhizo-C- and Micro-C-treated soils (Fig. 2b).

251   The cumulative mineralization of substrate-derived ^{13}C was more rapid at the beginning of the

252   incubation and followed a single exponential model (Fig. S1), and at the end of the incubation, we

253   found that the percentage of substrate-derived C that was mineralized was highest in Root-C-treated

254   soils (45.4%), followed by Shoot-C- (31.9%), Rhizo-C- (7.9%), and Micro-C-treated (7.7%) soils. In

255   the treatments of Rhizo-C, and Micro-C, about 0.3% and 0.1% of the total C emission were derived

256   from labelled rhizodeposited C and microbial assimilated C. In addition, the size of the bioavailable

257   labelled-substrate C pool in the Shoot-C- and Root-C-treated soils was 34.2 and 46.2%, respectively,

258   which was 4- to 5-fold larger than that of the Micro-C- (9.7%) and Rhizo-C-treated (7.8%) soils, and

259   the mean residence times (MRT) of the Shoot-C-, Root-C-, Rhizo-C-, and Micro-C-treated soils were

260   39.5, 50.3, 66.2, and 195 d, respectively (Table 2).

261

262   **3.2 Priming effect of Shoot-C and Root-C on CO_2 and CH_4 emission**

263   During incubation, the emission rates of CO_2 and CH_4 from control soils ranged from 4.7 to 15.9 mg

264   kg^{-1} d^{-1}. The addition of Shoot-C and Root-C increased total C emissions from native SOC up to 11.4

265   and 2.3 times than that of the untreated soils by day 20, respectively, and the PE persisted to the end of

266   incubation period. The C emission from native SOC increased linearly during the first 20 d, and then

267   decreased rapidly (Fig. 3). Furthermore, the PE of Shoot-C peaked at 378% after 20 d of incubation and

268   decreased to 52% by the end of the incubation, whereas the PE of Root-C peaked at 43% after 50 d of

269   incubation and then decreased to 2.9%. Thus, the positive PE of Shoot-C was clearly stronger than that

270   of Root-C, especially since the PE of Root-C was insignificant (Fig. 4).

271

272   **3.3 Mineralization of soil organic carbon in Rhizo-C- and Micro-C-treated soils**

273   The total C emissions of Rhizo-C- and Micro-C-treated-soils increased significantly from 116 mg kg^{-1}

274   and 81 mg kg^{-1} after 10 d of incubation, respectively, to 1754 mg kg^{-1} and 1785 mg kg^{-1} by the end of

275   the incubation. The total C emission of Rhizo-C-treated soil was significantly higher than that of the

Micro-C-treated and untreated soil during the first 200 d of incubation; however, no significant differences were identified at the end of the incubation (Fig. 5a). In addition, the total ^{13}C emission derived from the labelled substrates was significantly higher for the Rhizo-C-treated soils than for the Micro-C-treated soils ($p < 0.05$; Fig. 5b). However, the cumulative C mineralization of neither the Rhizo-C- nor the Micro-C-treated soils was significantly different from that of untreated soils, which suggested that the rhizodeposits and microbe-assimilated C had no positive effect on the mineralization of native SOC.

4   Discussion

4.1 Mineralization of carbon substrates in paddy soil

The effluxes of both CO_2 and CH_4 from soils treated with ^{13}C-labelled substrates exhibited a rapid increase at the beginning of the incubation, followed by a slow decrease (Fig. 1), which indicated that microbes prefer fresh C substrates over native SOC (Yuan et al., 2012c), as has been reported by previous studies on the decomposition of fresh C substrates in both paddy and upland soils (Lu et al., 2003; Parshotam et al., 2000). In these systems, the initial rapid decomposition is due to the addition of easily degradable organic C in the added substrates, such as starch and other labile compounds. Then, after the exhaustion of labile C from the added substrates, more recalcitrant components, such as cutin and lignin, from both the added substrates and native SOM, are utilized, along with native mineral-stabilized SOC (Baumann et al., 2009). The transition could also involve an alteration in species dominance, with rapidly proliferating bacteria using more available compounds during the early stages of decomposition and slower-growing fungi using the more recalcitrant components during later stages (Baumann et al., 2009; Brant et al., 2006).

Both CO_2 and CH_4 efflux are important components of the C cycle in paddy soils and represent a major proportion of the C released by microbial decomposition (Yuan et al., 2012c), and the results of the present study suggest that the mineralization of shoot- and root-derived ^{13}C was ~3-4 times higher than that of rhizodeposit- and microbe-derived ^{13}C (i.e., Root-C > Shoot-C > Rhizo-C > Micro-C; Fig. 2). The present study also found that the percentage of root-derived ^{13}C recovered as CO_2 was 1.6-fold higher than that of shoot-derived ^{13}C recovered as CO_2. This suggests that root residue was more easily decomposed, a conclusion that was also supported by the higher $^{13}CO_2$ efflux of Root-C-treated soils.

However, the C mineralization rates of Rhizo-C- and Micro-C-treated soils were much slower, and the MRTs of Rhizo-C- and Micro-C-treated soils were 2- to 4-fold higher than those of Shoot-C- and Root-C-treated soils. Presumably, this resulted from the formation of mineral-associated organic matter during the labelling period that was well protected from microbial degradation and had a slow turnover rate (Basler et al., 2015; Mikutta et al., 2014; Saidy et al., 2012; Schurig et al., 2013). Another possible reason for this observation is that most of the C in Rhizo-C- and Micro-C-treated soils was not mineralized to CO_2 but, instead, underwent intensive internal recycling (Gunina and Kuzyakov, 2015; Knowles et al., 2010). The easily available substrate-derived C could be incorporated into metabolic products, such as sugars, carboxylic acids, and amino acids, which in turn are used to build up stable cell membranes, cell walls, or polymers (Apostel et al., 2015; Gunina et al., 2014). Microorganisms are also associated with minerals and, thus, are involved in the formation of occluded particulate organic matter and mineral-associated organic matter (Basler et al., 2015, Schurig et al., 2013), the latter of which is considered especially stable.

4.2 Effect of carbon substrates on native SOC mineralization

In the present study, the emission of CO_2 and CH_4 by Shoot-C- and Root-C-treated soils during the first 50 d were mainly derived from plant residue C, after which the relative contribution of native SOC increased. For Shoot-C, a positive PE was observed over the entire incubation period, whereas that of Root-C was only significant during early stages of the incubation (Fig. 4). These results support previous reports that the initial phase of rapid decomposition results from the addition of easily degraded organic C and other available nutrients with the residues that promote both microbial activity and SOC decomposition (Chen et al., 2014). The compounds decomposed during the slower phase were less available for microbial growth, and as a result of C limitation, most of the available C was likely incorporated into cells and converted to storage compounds, rather than used for growth or respiration (Lu et al., 2003; Brant et al., 2006). However, the extracellular enzymes generated to degrade recalcitrant C substrates might be more effective in decomposing SOC at later stages of incubation, leading to a positive PE (Chen et al., 2014). In addition, the two phases of exogenous C decomposition and the mechanisms of PE simultaneously influence the strength and extent of native SOC mineralization (Chen et al., 2014; Ye et al., 2015).

334   Both Rhizo-C and Micro-C augmented the C content of paddy soil (1.89 and 1.90%, respectively)

335   over that of the untreated soil (1.81%), although the C emissions of Rhizo-C- and Micro-C-treated soils

336   were similar to those of untreated soil. However, about 0.3% and 0.1% of the total C emission were

337   derived from labelled rhizodeposited C and microbial assimilated C, respectively. The results suggested

338   that rhizodeposits and microbe-assimilated C input failed to stimulate the mineralization of native SOC

339   and, instead, resulted in negative priming. Therefore, it seems that Rhizo-C and Micro-C protect native

340   SOC and increase the organic C storage of paddy soil (Ge et al., 2012; Li and Yagi, 2004; Gunina et al.,

341   2015). In addition, the lower C contents of Rhizo-C and Micro-C, compared to those Shoot-C and

342   Root-C, may reflect the different behaviours of the organic C substrates in the soil. Roots and shoots,

343   for example, enter the soil as particulate and unprotected organic matter, which is highly available for

344   microorganism uptake and assimilation (i.e., 31.9% and 45.4%, respectively), and were mineralized

345   within the 300-d incubation period (Fig. S1). Meanwhile, rhizodeposits consist mostly of low

346   molecular weight sugars and acids that are highly bioavailable (Lu et al., 2002), and the relatively long

347   MRTs of Rhizo-C (Table 2) suggests that the C was stabilized during the incubation, either by

348   adsorption or by microbial metabolism and recycling (Lu et al., 2002; Gunina et al., 2014; Schurig et

349   al., 2013). Micro-C also exhibited long MRTs in the incubation experiment (Table 2), which coincided

350   with the observation that microbial residues accumulated in the soil (Schurig et al., 2013).

351

352   5   Conclusions

353   In the present study, Root-C-treated soils exhibited the highest rate of C mineralization, followed by

354   Shoot-C-, Rhizo-C-, and Micro-C-treated soils, whereas the opposite trend was observed for MRT. By

355   the end of 300-d incubation, Shoot-C-treated soils exhibited higher total mineralization and positive

356   PEs, whereas Root-C failed to exhibit a significant priming effect. Although plant residues are widely

357   used for improving soil fertility, their contribution to SOC assimilation is inefficient, and their use also

358   contributes to the emission of greenhouse gasses. However, the present study demonstrates that both

359   rhizodeposits and microbe-assimilated C can reduce native SOC decomposition and may more

360   effectively contribute to the stability and sequestration of soil C.

361

371

References

Apostel, C., Dippold, M., Kuzyakov, Y.: Biochemistry of hexose and pentose transformations in soil analyzed by position-specific labeling and ^{13}C-PLFA, Soil Biol. Biochem., 80, 199-208, 2015.

Basler, A., Dippold, M., Helfrich, M., Dyckmans, J.: Microbial carbon recycling: An underestimated process controlling soil carbon dynamics–Part 2: A C3-C4 vegetation change field labelling experiment, Biogeosciences, 12(21), 6291-6299, 2015.

Bastida, F., Torres, I. F., Hernández, T., Bombach, P., Richnow, H. H., García, C.: Can the labile carbon contribute to carbon immobilization in semiarid soils? Priming effects and microbial community dynamics, Soil Biol. Biochem., 57, 892-902, 2013.

Baumann, K., Marschner, P., Smernik, R. J., Baldock, J. A.: Residue chemistry and microbial community structure during decomposition of eucalypt, wheat and vetch residues, Soil Biol. Biochem., 41, 1966-1975, 2009.

Blagodatskaya, E., Blagodatsky, S. A., Anderson, T. H., Kuzyakov, Y.: Priming effects in Chernozem induced by glucose and N in relation to microbial growth strategies, Appl. Soil Ecol., 37, 95-105, 2007.

Blagodatskaya, E., Khomyakov, N., Myachina, O., Bogomolova, I., Blagodatsky, S., Kuzyakov, Y.: Microbial interactions affect substrates of priming induced by cellulose, Soil Biol. Biochem., 74, 39-49, 2014.

Blagodatsky, S., Blagodatskaya, E., Yuyukina, T., Kuzyakov, Y.: Model of apparent and real priming effects: Linking microbial activity with soil organic matter decomposition, Soil Biol. Biochem., 42(8), 1275-1283, 2010.

Brant, J. B. Sulzman, E. W. Myrold, D. D.: Microbial community utilization of added carbon substrates in response to long-term carbon input manipulation, Soil Biol. Biochem., 38 (8) 2219-2232, 2006.

Chen, R., Senbayram, M., Blagodatsky, S., Myachina, O., Dittert, K., Lin, X., Blagodatskaya, E., Kuzyakov, Y.: Soil C and N availability determine the priming effect: microbial N mining and stoichiometric decomposition theories, Global Change Biol., 20(7), 2356-2367, 2014.

16

399 Conrad, R., Klose, M., Yuan, Q., Lu, Y., Chidthaisong, A.: Stable carbon isotope fractionation,

400 carbon flux partitioning and priming effects in anoxic soils during methanogenic degradation of

401 straw and soil organic matter, Soil Biol. Biochem., 49, 193-199, 2012.

402 Creamer, C. A., de Menezes, A. B., Krull, E. S., Sanderman, J., Newton-Walters, R., Farrell, M.:

403 Microbial community structure mediates response of soil C decomposition to litter addition and

404 warming, Soil Biol. Biochem., 80, 175-188, 2015.

405 Ge, T. D., Wu, X. H., Chen, X. J., Yuan, H. Z., Zou, Z., Li, B. Z., Zhou, P., Liu, S. L., Tong, C. L.,

406 Brookes, P., Wu, J. S.: Microbial phototrophic fixation of atmospheric CO_2 in China subtropical

407 upland and paddy soils, Geochim. Cosmochim. Acta., 113, 70-78, 2013.

408 Ge, T. D., Yuan, H. Z., Zhu, H. H., Wu, X. H., Nie, S. A., Liu, C., Tong, C. L., Wu, J. S., Brookes,

409 P.: Biological carbon assimilation and dynamics in a flooded rice – Soil system, Soil Biol.

410 Biochem., 48, 39-46, 2012.

411 Glanville, H., Rousk, J., Golyshin, P., Jones, D. L.: Mineralization of low molecular weight

412 carbon substrates in soil solution under laboratory and field conditions, Soil Biol. Biochem., 48,

413 88-95, 2012.

414 Gunina, A., Dippold, M. A., Glaser, B., Kuzyakov, Y.: Fate of low molecular weight organic

415 substrates in an arable soil: From microbial uptake to utilisation and stabilisation, Soil Biol.

416 Biochem., 77, 304-313, 2014.

417 Gunina, A., Kuzyakov, Y.: Sugars in soil and sweets for microorganisms: Review of origin,

418 content, composition and fate, Soil Biol. Biochem., 90, 87-100, 2015.

419 Hooker, B., Morris, T., Peters, R., Cardon, Z.: Long-term effects of tillage and corn stalk return on

420 soil carbon dynamics, Soil Sci. Soc. Am. J., 69(1), 188-196, 2005.

421 Hu, L. L., Su, Y. R., He, X. Y., Wu, J. S., Zheng, H., Li, Y., Wang, A.: Response of soil organic

422 carbon mineralization in typical Karst soils following the addition of ^{14}C-labeled rice straw and

423 CaCO$_3$, J. Sci. Food Agric., 92(5), 1112-1118, 2012.

424 Huo, L. J., Ji, X. H., Wu, J. M., Peng, H., Zhu, J.: Effects of applications of exogenous organic

425 carbon on methane emissions and oxidizable organic carbon in paddy soil, Res. Agric. Modern.,

426 34(4), 496-501, 2013. (English abstract in Chinese)

427   Jones, D. L., Edwards, A. C.: Influence of sorption on the biological utilization of two simple

428   carbon substrates, Soil Biol. Biochem., 30(14), 1895-1902, 1998.

429   Johnson, J. M. F., Allmaras, R. R., Reicosky, D. C.: Estimating substrate carbon from crop

430   residues, roots and rhizodeposits using the national grain-yield database, Agron. J., 98(3), 622-636,

431   2006

432   Kisselle, K. W., Garrett, C. J., Fu, S., Hendrix, P. F., Crossley Jr, D. A., Coleman, D. C., Potter, R.

433   L.: Budgets for root-derived C and litter-derived C: comparison between conventional tillage and

434   no tillage soils, Soil Biol. Biochem., 33(7-8), 1067-1075, 2001.

435   Knowles, T. D. J., Chadwick, D. R., Bol, R., Evershed, R. P.: Tracing the rate and extent of N and

436   C flow from ^{13}C, ^{15}N-glycine and glutamate into individual de novo synthesized soil amino acids,

437   Org. Geochem., 41(12), 1259-1268, 2010.

438   Kuzyakov, Y.: Priming effects: Interactions between living and dead organic matter, Soil Biol.

439   Biochem., 42(9), 1363-1371, 2010.

440   Kuzyakov, Y., Bol, R.: Substrates and mechanisms of priming effect induced in two grassland

441   soils amended with slurry and sugar, Soil Biol. Biochem., 38(4), 747-758, 2006.

442   Kuzyakov, Y., Friedel, J. K., Stahr, K.: Review of mechanisms and quantification of priming

443   effects, Soil Biol. Biochem., 32(11-12), 1485-1498, 2000.

444   Kuzyakov, Y., Leinweber, P., Sapronov, D., Eckhardt, K. U.: Qualitative assessment of

445   rhizodeposits in non-sterile soil by analytical pyrolysis, J. Plant Nutr. Soil Sci., 166(6), 719-723,

446   2003.

447   Kuzyakov, Y., Siniakina, S. V., Ruehlmann, J., Domanski, G., Stahr, K.: Effect of nitrogen

448   fertilisation on below-ground carbon allocation in lettuce, J. Sci. Food Agric., 82(13), 1432-1441,

449   2002.

450   Lal, R.: Soil Carbon Sequestration Impacts on Global Climate Change and Food Security, Science,

451   304(5677), 1623-1627, 2004.

452   Li, Z., Yagi, K.: Rice root-derived carbon input and its effect on decomposition of old soil carbon

453   pool under elevated CO_2, Soil Biol. Biochem., 36(12), 1967-1973, 2004.

454   Lu, Y. H., Watanabe, A., Kimura, M.: Contribution of plant-derived carbon to soil microbial

455   biomass dynamics in a paddy rice microcosm, Biol. Fertil. Soil., 36(2), 136-142, 2002.

456   Lu, Y. H., Watanabe, A., Kimura, M.: Carbon dynamics of rhizodeposits, root- and shoot-residues

457   in a rice soil, Soil Biol. Biochem., 35(9), 1223-1230, 2003.

458   Mikutta, R., Lorenz, D., Guggenberger, G., Haumaier, L., Freund, A.: Properties and reactivity of

459   Fe-organic matter associations formed by coprecipitation versus adsorption: Clues from arsenate

460   batch adsorption, Geochim. Cosmochim. Acta., 144, 258-276, 2014.

461   Molina, J. A. E., Clapp, C. E., Linden, D. R., Allmaras, R. R., Layese, M. F., Dowdy, R. H.,

462   Cheng, H. H.: Modeling the incorporation of corn (Zea mays L.) carbon from roots and

463   rhizodeposition into soil organic matter, Soil Biol. Biochem., 33(1), 83-92, 2001.

464   Nguyen, C.: Rhizodeposition of organic C by plants: mechanisms and controls, Agron., 23(5-6),

465   375-396, 2003.

466   Parshotam, A., Saggar, S., Searle, P. L., Daly, B. K., Sparling, G. P., Parfitt, R. L.: Carbon

467   residence times obtained from labeled ryegrass decomposition in soils under contrasting

468   environmental conditions, Soil Biol. Biochem., 32(1), 75-83, 2000.

469   Paul, S., Veldkamp, E., Flessa, H.: Differential response of mineral-associated organic matter in

470   tropical soils formed in volcanic ashes and marine Tertiary sediment to treatment with HCl,

471   NaOCl, and $Na_4P_2O_7$, Soil Biol. Biochem., 40(7), 1846-1855, 2008.

472   Phillips, D., Newsome, S.D., Gregg, J.: Combining substrates in stable isotope mixing models:

473   alternative methods, Oecologia, 144(4), 520-527, 2005.

474   Qiao, N., Schaefer, D., Blagodatskaya, E., Zou, X., Xu, X., Kuzyakov, Y.: Labile carbon retention

475   compensates for CO2 released by priming in forest soils, Global Change Biol., 20, 1943-1954,

476   2014.

477   Saidy, A. R., Smernik, R. J., Baldock, J. A., Kaiser, K., Sanderman, J., Macdonald, L. M.: Effects

478   of clay mineralogy and hydrous iron oxides on labile organic carbon stabilisation, Geoderma, 173,

479   104-110, 2012.

480 Schurig, C., Smittenberg, R. H., Berger, J., Kraft, F., Woche, S. K., Goebel, M. O., Heipieper, H.

481 J., Miltner, A., Kaestner, M.: Microbial cell-envelope fragments and the formation of soil organic

482 matter: a case study from a glacier fore field, Biogeochemistry, 113(1), 595–612, 2013.

483 Sodano, M., Said-Pullicino, D., Fiori, A. F., Catoni, M., Martin, M., Celi, L.: Sorption of paddy

484 soil-derived dissolved organic matter on hydrous iron oxide-vermiculite mineral phases,

485 Geoderma, 261, 169–177, 2016.

486 Tian, J., Dippold, M., Pausch, J., Blagodatskaya, E., Fan, M., Li, X., Kuzyakov, Y.: Microbial

487 response to rhizodeposition depending on water regimes in paddy soils, Soil Biol. Biochem., 65,

488 195-203, 2013.

489 Wang, W., Lai, D. Y. F., Wang, C., Pan, T., Zeng, C.: Effects of rice straw incorporation on active

490 soil organic carbon pools in a subtropical paddy field, Soil Till. Res., 152, 8-16, 2015.

491 Weintraub, M., Scott-Denton, L., Schmidt, S., Monson, R.: The effects of tree rhizodeposition on

492 soil exoenzyme activity, dissolved organic carbon, and nutrient availability in a subalpine forest

493 ecosystem, Oecologia, 154(2), 327-338, 2007.

494 Wild, B., Schnecker, J., Alves, R. J. E., Barsukov, P., Bárta, J., Čapek, P., Gentsch, N., Gittel, A.,

495 Guggenberger, G., Lashchinskiy, N., Mikutta, R., Rusalimova, O., Šantrůčková, H., Shibistova, O.,

496 Urich, T., Watzka, M., Zrazhevskaya, G., Richter A.: Input of easily available organic C and N

497 stimulates microbial decomposition of soil organic matter in arctic permafrost soil. Soil Biol.

498 Biochem., 75, 143-151, 2014.

499 Ye, R., Doane, T. A., Morris, J., Horwath, W. R.: The effect of rice straw on the priming of soil

500 organic matter and methane production in peat soils, Soil Biol. Biochem., 81, 98-107, 2015.

501 Yuan, H. Z., Ge, T. D., Chen, C., O'Donnell, A. G., Wu, J. S.: Significant role for microbial

502 autotrophy in the sequestration of soil carbon, Appl. Environ. Microbiol., 78(7), 2328-2336, 2012.

503 Yuan, H. Z., Ge, T. D., Wu, X., Liu, S., Tong, C. L., Qin, H., Wu, M., Wei, W. X., Wu, J. S.:

504 Long-term field fertilization alters the diversity of autotrophic bacteria based on the

505 ribulose-1,5-biphosphate carboxylase/oxygenase (RubisCO) large-subunit genes in paddy soil,

506 Appl. Microbiol. Biotechnol., 95(4), 1061-1071, 2012.

507   Yuan, Q., Pump, J., Conrad, R.: Straw application in paddy soil enhances methane production also

508   from other carbon substrates, Biogeosciences, 11(2), 237-246, 2014.

509   Zhang, G., Yu, H., Fan, X., Liu, G., Ma, J., Xu, H.: Effect of rice straw application on stable

510   carbon isotopes, methanogenic pathway, and fraction of CH_4 oxidized in a continuously flooded

511   rice field in winter season, Soil Biol. Biochem., 84, 75-82, 2015.

512

513 **Tables**

514 **Table 1.** Carbon (C) and atomic ^{13}C contents and amount of ^{13}C added of untreated bulk soil and soils

515 treated with one of four labelled C substrates.

	Bulk soil	Shoot-C	Root-C	Rhizo-C	Micro-C
C content (%)	1.80 ±0.12	40.50 ±2.13	28.60 ±1.15	1.89 ±0.12	1.90 ±0.11
Atomic ^{13}C (%)	1.08 ±0.02	5.78 ±0.09	4.43 ±0.07	1.16 ±0.03	1.11 ±0.02
Total excess of ^{13}C (mg)	-	11.43±0.52	5.75 ±0.41	1.61 ±0.06	0.49 ±0.05

516 Bulk soil, unplanted control soil; Shoot-C, paddy soil supplemented with ^{13}C-labelled shoot residue;

517 Root-C, paddy soil supplemented with ^{13}C-labelled root residue;Rhizo-C, paddy soil supplemented

518 with ^{13}C-labelled rhizodeposits; Micro-C, paddy soil supplemented with ^{13}C-labelled

519 microbe-accumulated C.

520

521 **Table 2.** Bioavailable labelled-substrate C pool, mean residence time (MRT), and half-life of

522 cumulative ^{13}C recovery in CO_2 and CH_4 of soils incubated with one of four labelled C substrates.

Treatment	Size (%)	MRT (d)	Half-life (d)	R^2
Shoot-C	32.4 ±0.56	39.5 ±0.63	27.4 ±0.55	0.99
Root-C	44.9 ±1.12	50.3 ±0.71	34.7 ±0.62	0.99
Rhizo-C	7.3 ±0.38	66.2 ±0.92	46.4 ±1.31	0.98
Micro-C	9.1 ±0.44	195 ±1.52	136 ±1.66	0.98

523 The size of bioavailable labelled-substrate C pool (% initial ^{13}C), MRT, and R^2 were calculated based

524 on Fig. 1S. Shoot-C, paddy soil supplemented with ^{13}C-labelled shoot residue; Root-C, paddy soil

525 supplemented with ^{13}C-labelled root residue; Rhizo-C, paddy soil supplemented with ^{13}C-labelled

526 rhizodeposits; Micro-C, paddy soil supplemented with ^{13}C-labelled microbe-accumulated C.

527 **Figures captions**

528 **Figure 1.** $^{13}CO_2$ (**c**) and $^{13}CH_4$ (**d**) efflux per day over the 300-d incubation period. Values and error

529 bars represent mean % initial $^{13}C \pm SE$ (n = 4). Shoot-C, unlabelled paddy soil supplemented with

530 ^{13}C-labelled shoot residue; Root-C, unlabelled paddy soil supplemented with ^{13}C-labelled root residue;

531 Rhizo-C, paddy soil containing ^{13}C-labelled rhizodeposits; Micro-C, paddy soil containing ^{13}C-labelled

532 microbe-accumulated C.

533

534 **Figure 2.** Cumulative $^{13}CO_2$ (**a**) and $^{13}CH_4$ (**b**) emissions over the 300-d incubation period. Values and

535 error bars represent mean % of initial $^{13}C \pm SE$ (n = 4). Shoot-C, unlabelled paddy soil supplemented

536 with ^{13}C-labelled shoot residue; Root-C, unlabelled paddy soil supplemented with ^{13}C-labelled root

537 residue; Rhizo-C, paddy soil containing ^{13}C-labelled rhizodeposits; Micro-C, paddy soil containing

538 ^{13}C-labelled microbe-accumulated C.

539

540 **Figure 3.** Rates of CO_2-C and CH_4-C emissions from Shoot-C- (**a**) and Root-C-treated (**b**) soils over

541 the 300-d incubation period. Values and error bars represent means $\pm SE$ (n = 4). Shoot-C, ^{13}C-labelled

542 shoot residue; Root-C, ^{13}C-labelled root residue; SOC, soil organic carbon; CK, unlabelled and

543 unplanted soil without supplementation.

544

545 **Figure 4.** Priming effect of ^{13}C-labelled plant residues over the 300-d incubation period. Values and

546 error bars represent means $\pm SE$ (n = 4). Shoot-C, unlabelled paddy soil supplemented with ^{13}C-labelled

547 shoot residue; Root-C, unlabelled paddy soil supplemented with ^{13}C-labelled root residue.

548

549 **Figure 5.** Total C (**a**) and ^{13}C (**b**) emission by ^{13}C-labelled Rhizo-C- and Micro-C-accumulated

550 C-treated soils over the 300-d incubation period. Values and error bars represent means $\pm SE$ (n = 4).

551 Different letters indicate significant differences at $p < 0.05$ (Duncan multiple range test). Rhizo-C,

552 paddy soil containing ^{13}C-labelled rhizodeposits; Micro-C, paddy soil containing ^{13}C-labelled

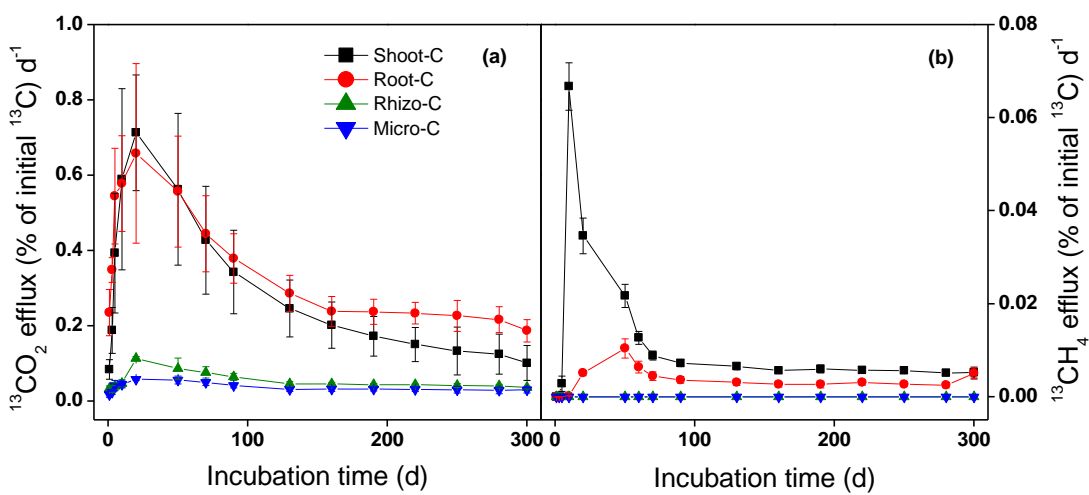553 microbe-accumulated C; CK, unlabelled and unplanted soil without supplementation.
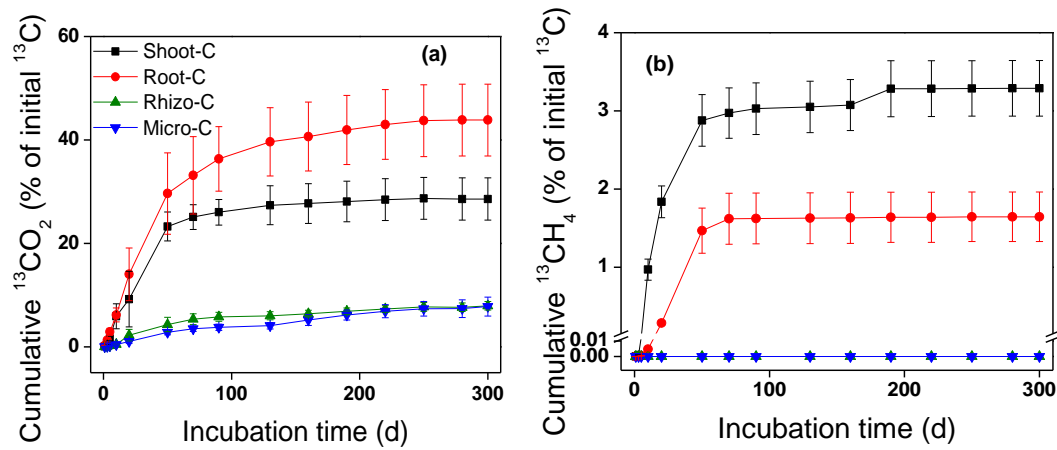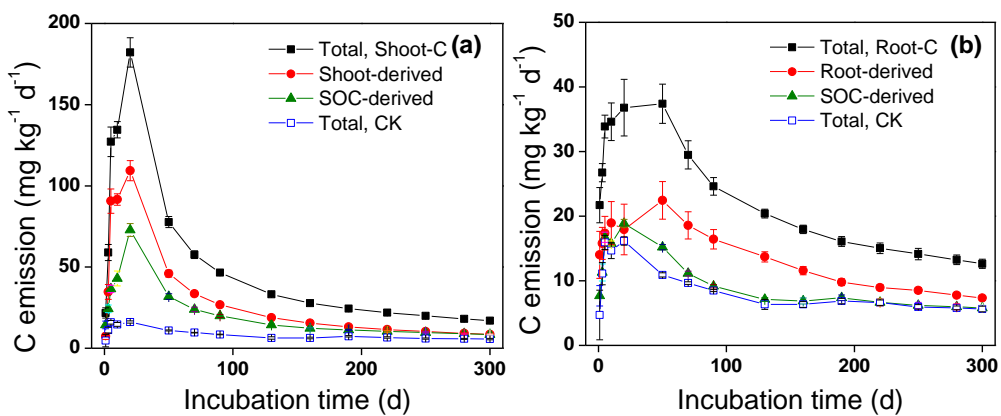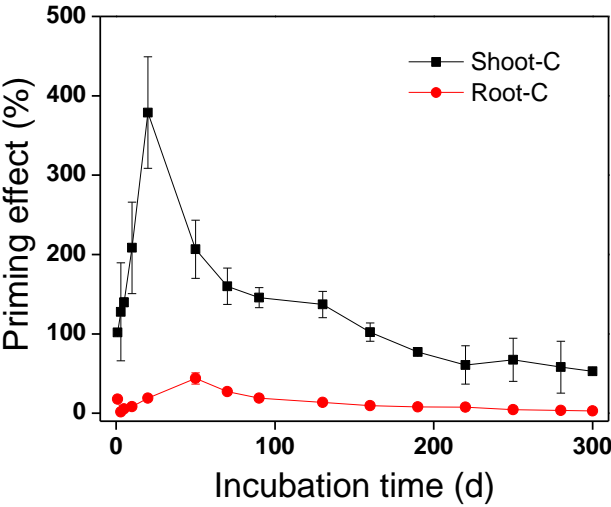
554

555 **Figure 1**

556

557

558   **Figure 2**

559

560

561 **Figure 3**

562

563

564 **Figure 4**

565

566

567   **Figure 5**

568